Two New Members of the Dimeric β-Linked Face-to-Face Porphyrin Family: FTF4* and FTF3[1]

James P. Collman,* C. Susana Bencosme, Craig E. Barnes, and Bryan D. Miller

Contribution from the Department of Chemistry, Stanford University. Stanford, California 94305. *Received August 9, 1982*

Abstract: Two new β-linked "face-to-face" porphyrin dimers have been synthesized and characterized by ^1H NMR, UV–visible, and mass spectroscopic analyses. These compounds have the two linking amide bridges between the porphyrin rings located on opposite β-pyrrolic carbons, with the amide carbonyl groups directly attached to the porphyrin rings. The interporphyrin separation constitutes the major structural difference between the two compounds: four-atom bridges in one of them (FTF4*) and three-atom bridges in the other (FTF3). NMR spectroscopy reveals the presence of only one diastereoisomer in both cases.

Improvements in the efficiency of economical oxygen cathodes remain an important challenge in fuel cell systems. As an approach to the design and synthesis of an electrocatalyst for the rapid four-electron reduction of molecular oxygen to water,[2,3] we have already reported the synthesis and characterization of a series of covalently linked face-to-face porphyrin dimers.[4] These compounds have the two porphyrin macrocycles linked by bridges located at either the transverse meso or β positions of the ring. This forces the two cyclophane planes to lie parallel to each other; thus, their metal derivatives can interact simultaneously in the binding and subsequent reduction of dioxygen.

In the β-amide-linked porphyrin dimers that have been examined to date, it has been observed that the narrower the gap between the cyclophane rings, the stronger the electronic interaction between the porphyrin groups. This is manifest in their ^1H NMR and UV–visible spectra and in the formal potentials of their cobalt derivatives (Table I).[2b]

Using the technique of rotating-disk voltammetry,[5,6] we have previously reported on the catalytic activity of a number of mono- and dimetal derivatives of these molecules toward the electrochemical reduction of dioxygen. Only the dicobalt derivative of the β-linked dimer with two four-atom bridges (Co_2(FTF4)) Figure 1 was found to achieve four-electron reduction of O_2 to H_2O.[2b,7,8] The cobalt derivative of FTF6 (**1a**) shows monomer-like catalytic activity. The two cobalt centers appear to act independently in binding and catalyzing the reduction of dioxygen. Hydrogen peroxide is the sole reduction product.[2b]

Two different kinds of binary porphyrins with five-atom bridges have been synthesized previously: FTF5 (**2a**) and FTF5* (**3a**).[7b] The only structural difference between these two isomers is the location of the amide groups in the linking bridges. The cobalt derivatives of both FTF5 (**2b**) and FTF5* (**3b**) show catalytic activity that differs from that of Co_2(FTF6) (**1b**). Both isomers promote simultaneous two-electron and four-electron pathways for the reduction of dioxygen. It is noteworthy that the cobalt derivative of FTF5* (**3b**), which has the carbonyl groups closer to the porphyrin ring, is a better catalyst than its isomer, Co_2(FTF5) (**2b**) in that the dioxygen reduction occurs at more positive potentials, with larger total currents corresponding to less production of hydrogen peroxide.

For the still more closely linked dimer Co_2(FTF4) (**4b**), the catalytic four-electron reduction of dioxygen to water is the predominant reaction. The catalytic half-wave potential (+0.7 V) is also considerably more positive than those of the other β-bridged porphyrin dimers, although still far from the reversible O_2/H_2O potential (+1.23 V).

Analysis of the physical properties presented in Table I for the dimers and their cobalt derivatives suggests possible strategies for optimizing the catalytic efficiency. One approach is to attempt to reproduce the behavioral pattern observed with Co_2(FTF5) and Co_2(FTF5*) in the four-atom-bridged homologues by synthesizing a new dimer, with the carbonyl groups of the amide directly attached to one of the porphyrin rings (FTF4*, **5a**) (Figure 1). The electron-withdrawing effect of the conjugated carbonyl groups should remove electron density from the pyrrolic nitrogens, making them less basic. This effect should then be reflected in a more positive formal potential for the cobalt center coordinated to this porphyrin ring. We expected that this positive shift of the potential where the cobalt is reduced might produce a similar shift in the potential where dioxygen reduction occurs. Such a positive shift was observed when the dicobalt derivative of FTF4 was chlorinated in the meso position.[9]

Another possible approach to improve the performance of the catalyst is to decrease the interporphyrin separation. This has now been achieved by synthesizing a new fact-to-face porphyrin dimer with two three-atom bridges (FTF3, **6a**).

The small separation between the two porphyrin rings in this molecule may prevent the formation of the intermediate cobalt–dioxygen adduct that we believe is required for these catalysts to achieve the four-electron reduction of dioxygen.[2b] Thus, while Co_2(FTF3) may not be as good a catalyst as Co_2(FTF4) for reducing O_2 to H_2O, its catalytic behavior seemed worth exploring from a mechanistic point of view.

The synthesis and characterization of FTF4* and FTF3 are described in this report. The electrochemical studies of their cobalt derivatives as potential catalysts for the reduction of O_2 are reported elsewhere.[8]

Synthesis. The synthetic scheme leading to FTF4* (**5a**) and FTF3 (**6a**) is shown in Figure 2. The porphyrin coupling reaction is carried out by slow addition of equimolar CH_2Cl_2 solutions of the corresponding β-substituted diamine **10** or **11** and acyl chloride

(1) This paper was abstracted from the Ph.D Thesis of C.S.B. Stanford University, 1982.

(2) (a) Collman, J. P.; Elliott, C. M.; Halbert, T. r.; Tovrog, B. S. *Proc. Natl. Acad. Sci. U.S.A.* **1977**, *74*, 18–22. (b) Collman, J. P.; Denisevich, P.; Konai, Y.; Marrocco, M.; Koval, C.; Anson, F. C. *J. Am. Chem. Soc.* **1980**, *102*, 6027–6036.

(3) van den Brink, F.; Barendrecht, E.; Visscher, W. *Recl. Trav. Chim. Pays-Bas* **1980**, *99*, 253 and references therein

(4) Collman, J. P.; Anson, F. C.; Bencosme, S.; Chong, A.; Collins, T.; Denisevich, P.; Evitt, E.; Geiger, T.; Ibers, J. A.; Jameson, G.; Konai, Y.; Koval, C.; Meier, K.; Oakley, R.; Pettman, R.; Schmittou, E.; Sessler, J. In "Organic Synthesis Today and Tomorrow" (IUPAC); Trost, B. M., Hutchinson, C. R., Eds.; Pergamon: Oxford, 1981; pp 29–45.

(5) Albery, W. S.; Hitchman, M. L. "Ring-Disk Electrodes"; Clarendon Press: Oxford, 1975; and references therein.

(6) Bard, A. J.; Faulkner, L. R. "Electrochemical Methods, Fundamentals and Applications"; Wiley: New York, 1980; p 280.

(7) (a) Collman, J. P.; Marrocco, M.; Denisevich, P.; Koval, C.; Anson, F. C. *J. Electroanal. Chem. Interfacial Electrochem.* **1979**, *101*, 117–122. (b) Denisevich, P., Ph.D. Thesis, Stanford University, 1979.

(8) Durand, R. R., Jr.; Bencosme, C. S.; Collman, J. P.; Anson, F. C. *J. Am. Chem. Soc.*, following paper in this issue.

(9) Collman, J. P.; Anson, F. C.; Barnes, C. E.; Bencosme, C. S.; Geiger, T.; Evitt, E. R.; Kreh, R. P.; Meier, K.; Pettman, R. B. *J. Am. Chem. Soc.*, first of four papers in this issue.

0002-7863/83/1505-2704$01.50/0

Table I

compound	electronic spectra: Soret	electronic spectra: band I	NMR, ppm: pyrr·NH	NMR, ppm: meso	Co^{III}/Co^{II} potentials: *a*	Co^{III}/Co^{II} potentials: *b*
diester monomer (**12**)	400	620	−3.75	10.10–10.16	0.35	0.76
FTF6	384	624	−6.2	9.0–9.4	0.53	
FTF5	381	627	−8.0, −8.3	8.7–8.9	0.50, 0.68	
FTF5*	380	626	−7.9, −8.0	8.7–8.9	0.46, 0.71	
FTF4	376	628	−8.15 (br)	8.69–8.91	0.47, 0.67	0.84–0.64
FTF4*	372	640 (sh)	−7.78, −7.81	8.78, 9.29		0.89–0.60
FTF3	370	644	−7.81, −7.93	8.90, 8.98		0.89–0.59

[a] Potentials measured in BzCN/0.2 M TBAP vs. Ag wire reference. Potential of ferrocene/ferrocinium couple vs. this reference was 0.40 ± 0.03 V. [b] Formal potential (vs. NHE) of the catalyst adsorbed on pyrolytic graphite in 1 M CF_3COOH.

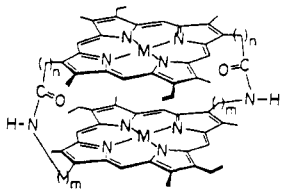

n = 2, m = 2: 1a, FTF6, M = 2H; 1b, Co_2FTF6, M = Co
n = 2, m = 1: 2a, FTF5, M = 2H; 2b, Co_2FTF5, M = Co
n = 1, m = 2: 3a, FTF5*, M = 2H; 3b, Co_2FTF5*, M = Co
n = 1, m = 1: 4a, FTF4, M = 2H; 4b, Co_2FTF4, M = Co
n = 0, m = 2: 5a, FTF4*, M = 2H; 5b, Co_2FTF4*, M = Co
n = 0, m = 1: 6a, FTF3, M = 2H; 6b, Co_2FTF3, M = Co

Figure 1. β-Linked face-to-face dimeric porphyrins.

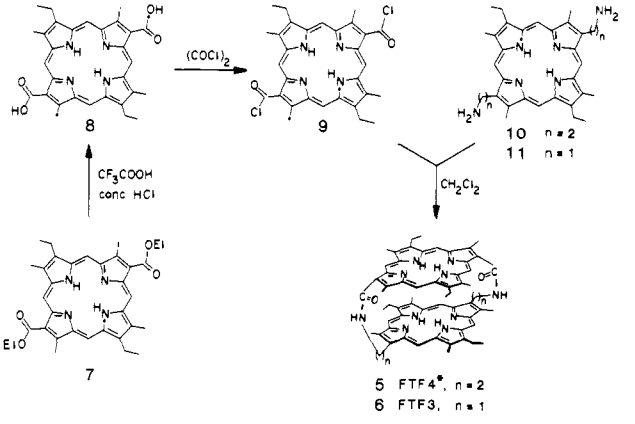

Figure 2. Synthetic scheme for the preparation of FTF4* and FTF3.

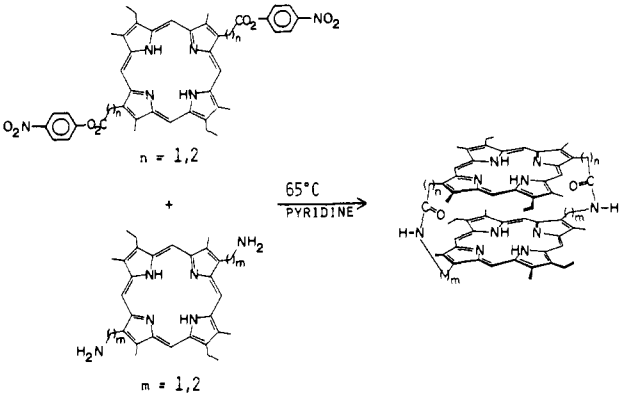

Figure 3. Synthesis of β-linked face-to-face porphyrin dimers.

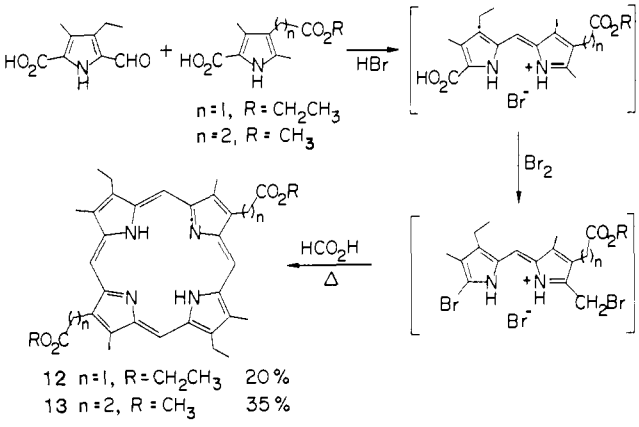

Figure 4. Synthesis of porphyrins with functional groups on transverse β-pyrrolic carbons.

9 into a flask containing dry methylene chloride. Simultaneous addition of the two reagents by means of a syringe pump, and high dilution conditions, minimize polymer formation. Monomeric diamine porphyrins **10** and **11** were obtained by treatment of the corresponding diacid precursors with NaN_3 in H_2SO_4, as previously described.[9] The acyl chloride **9** was obtained by treating the diacid **8** with oxalyl chloride.

The diacid **8** was prepared from acid hydrolysis of the Cl diethyl ester **7**. In the past, we have synthesized β-amide-linked face-to-face porphyrin dimers by coupling a di-*p*-nitrophenyl ester porphyrin monomer with the corresponding diamine (Figure 3). Attempts to synthesize the Cl di-*p*-nitrophenyl ester derivative failed, probably because of steric effects.

A key step in the entire synthesis was the preparation of the Cl diethyl ester porphyrin **7**. Porphyrins are usually derived from condensation of pyrroles. In the past, we have prepared the β-substituted diester porphyrins with two- and three-atom chains on transverse β-pyrrolic carbons, using a modified Fischer method as depicted in Figure 4.[2b,10] Nevertheless, electron-withdrawing groups directly attached to the β-pyrrolic carbons inhibit the pyrrole condensation to porphyrins via dipyrromethene intermediates.[11]

We have found, in effect, that the yield of the porphyrin synthesis decreased from C3 dimethyl ester **13** (35%) to the C2 diethyl ester **12** (20%). For the Cl diethyl ester **7**, traces of etioporphyrin constituted the only product. Therefore, in order to prepare **7** we found it necessary to investigate alternative syntheses. A scheme proceeding via dipyrromethane intermediates[12] was investigated and proved successful.

As outlined in Figure 5, the target porphyrin, **7**, was obtained by the self-condensation of the α-formyl, α′-free dipyrromethane of the appropriate substitution pattern, **17**. The dipyrromethane **17** was generated by deprotection of the thioacetal dipyrromethane **16** using mercuric oxide–boron trifluoride etherate in THF. Compound **16**, in turn, was the product from the condensation of the α-free pyrrole **14**,[13] with the acetoxymethyl pyrrole **15**.[14]

(10) We thank Prof. A. Battersby who kindly provided us, in advance of publication, the modified Fischer method for the porphyrin synthesis.

(11) Paine, J. B., III. In "The Porphyrins"; Dolphin, D., Ed.; Academic Press: New York, 1978; Vol IA, p 101.
(12) Clezy, P. S.; Fookes, C. J. R. *Aust. J. Chem.* **1974**, *27*, 371.

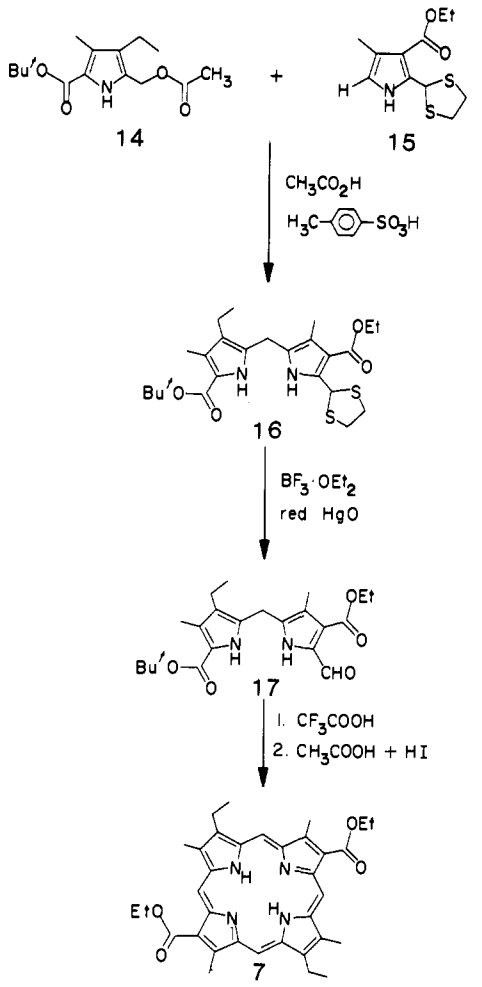

Figure 5. Synthesis of the C1 ethyl ester porphyrin **7**.

Table II. Electronic Spectral Data for "Face-to-Face" Porphyrins and Selected Monomeric Porphyrins in Methylene Chloride (λ_{max} in nm)

porphyrin	Soret	IV	III	II	I
FTF4 (4a)	376	502	544	572	626
FTF4* (5a)	372	507	548	578	640 (sh)
FTF3 (6a)	370	502 (sh)	536	566	644
C1 ethyl ester (7)	410	517	558	582	636
C2 ethyl ester (12)	400	498	536	566	620

UV–Visible Spectroscopy. Typical UV–visible spectra of porphyrins consist of an intense absorption band at approximately 400 nm, known as the Soret band, and four satellite bands, labeled as I, II, III, and IV, located in the visible region between 700 and 500 nm. The relative positions and intensities of these bands depend upon the nature and location of the substituents on the porphyrin ring. When the macrocycle has six or more alkyl groups in the β-pyrrolic positions, the visible bands have an intensity pattern such that IV > III > II > I, a so-called etio-type spectrum. This is the type of spectrum we have previously observed for all the monomeric precursors of our β-linked porphyrin dimers.[2b]

For the C1 ethyl ester porphyrin monomer **7** described here, however, a different spectrum is observed. Band III is more intense than the others, affording an oxorhodo spectrum (III > II > IV > I). These "rhodofying" groups also cause the absorptions to shift toward longer wavelengths. The Soret band has an asymmetric shape, with a shoulder at each side of the band. Similar phenomena have been observed for other porphyrins containing trans-β-carbonyl functions conjugated with the porphyrin ring.[15,16] A comparison of the UV–visible spectra of the C2 **12** and C1 **7** diethyl esters is displayed in Figure 6. A summary of the UV–visible spectral data of selected porphyrins is presented in Table II.

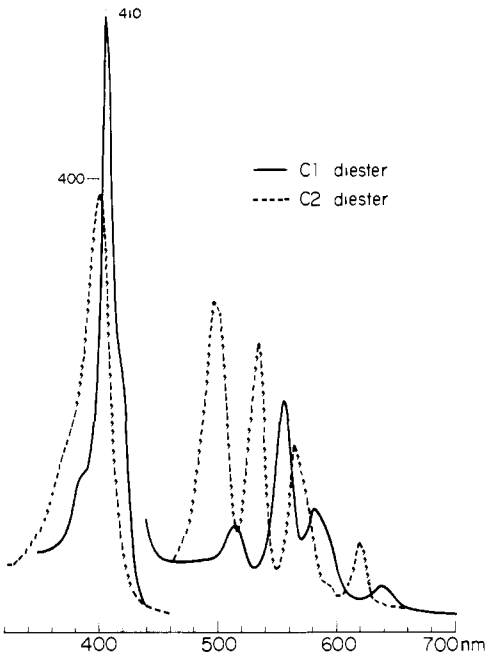

Figure 6. Comparison of the UV spectra of the C1 ethyl ester **7** and C2 ethyl ester **12**.

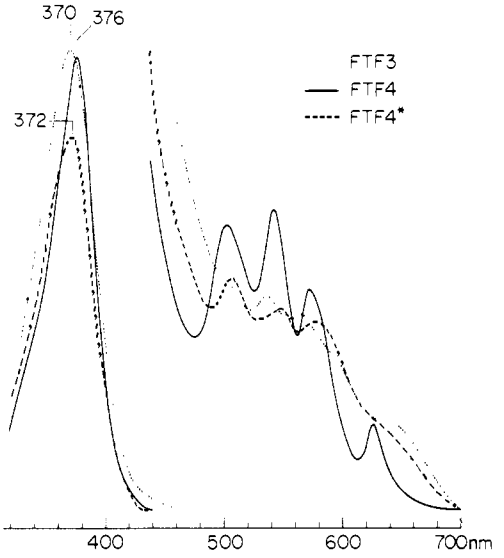

Figure 7. Comparison of the UV–vis spectra of FTF4 and FTF4*.

The two new face-to-face porphyrin dimers, FTF4* (**5a**) and FTF3 (**6a**), have UV–visible spectra that are substantially different from those observed for the other β-amide-linked dimers **1a**, **2a**, **3a**, **4a** (Figure 7). Both have blue-shifted Soret bands (FTF4*: λ_{max} 372 nm; FTF3: λ_{max} 370 nm) compared to FTF4 (λ_{max} 376 nm). Also, these bands are very broad, and the absorptions in the visible region are actually superimposed on the tails of the Soret bands. As a consequence, the visible bands are poorly resolved: they are red-shifted for FTF4* and blue-shifted for

(13) (a) Clezy, P. S.; Fookes, C. J. R.; Lien, D. Y. K.; Nichol, A. W.; Smithe, G. A. *Aust. J. Chem.* **1974**, *27*, 356. (b) Cavaleiro, J. A. S.; Gonsalves, A. M. d'A. R.; Kenner, G. W.; Smith, K. M. *J. Chem. Soc., Perkin Trans. 1* **1973**, 2471.

(14) Johnson, A. W.; Matehan, E.; Price, R.; Shaw, K. B. *J. Chem. Soc.* **1958**, 4256.

(15) Gouterman, M. In "The Porphyrins"; Dolphin, D., Ed.; Academic Press: New York, 1978; Vol IIIA, p 3.

(16) Smith, K. M. In "Porphyrins and Metalloporphyrins"; Smith, K. M., Ed.; Elsevier: Amsterdam, 1976; p 3.

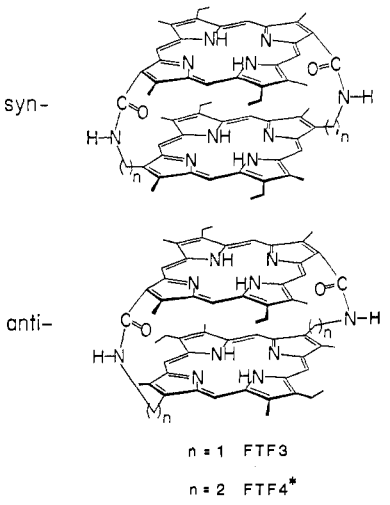

Figure 8. Syn and anti diastereoisomers of FTF3 and FTF4*.

FTF3, with respect to those for FTF4.

These qualitative spectral patterns and absorption shifts have proved useful in the identification of our porphyrin compounds. A more rigorous analysis of the electronic spectra is not presented in this paper.

^{1}H NMR Spectroscopy. The ^{1}H NMR spectrum of C1 ethyl ester porphyrin **7** is consistent with the structure assigned in Figure 3. It exhibits two meso proton signals, as expected for a porphyrin of C_2 symmetry. Similarly, two signals are obtained for the β-pyrrole methyl groups (δ 3.70, 3.94). The resonance arising from the internal pyrrolic NH in the C1 ester **7** is about the same (δ-3.76) as the C2 ethyl ester porphyrin **12** (δ−3.75). In contrast, the two meso proton peaks in **7** are shifted downfield and are well resolved as two singlets (δ 10.17 and 11.12). This is expected for porphyrins with conjugated carbonyl groups, as in compound **7**, because of an increase in the anisotropic shielding by the aromatic porphyrin ring. Representative ^{1}H NMR data for porphyrin monomers and dimers are presented in Table III.

The ^{1}H NMR results for FTF4* (**5a**) and FTF3 (**6a**) provide strong support for their cofacial formulation. Figure 8 shows that both dimers can exist in two possible diastereomeric forms, syn and anti, depending on the relative orientation of the two rings. In addition, each diastereomer would exist as a mixture of two enantiomers. Each diastereomer should have two sets of equivalent meso hydrogen atoms on each porphyrin ring. Thus, the presence of the two diastereomers would, in principle, lead to the observation of a maximum of eight signals for the eight nonequivalent meso protons. Such a mixture would also exhibit a maximum of eight proton signals for the β-methyl groups. The syn and anti diastereomers should have similar ^{1}H NMR spectra, but the chemical shifts and coupling constants of analogous substituents would be expected to be different.

Table III. Representative ^{1}H NMR Data for Porphyrin Monomers and Dimers

porphyrin	pyrrolic NH	H (meso)	CH_3 (ring)
monomers			
C2 ethyl ester (**12**)	−3.75	10.10, 10.16	3.67
C1 ethyl ester (**7**)	−3.76	10.17, 11.12	3.70, 3.94
dimers			
FTF4 (**4a**)	−8.14 (br)	8.70–8.91	3.58–3.60
FTF4* (**5a**)	−7.78, −7.81	8.78–9.29	3.60–3.74
FTF3 (**6a**)	−7.81, −7.93	8.90–8.98	3.65–3.90

A mixture of the two isomers should give rise to a more complex spectrum than that observed for FTF4*, which is presented in Figure 9. Only three peaks are observed in the chemical shift region corresponding to the meso protons (δ 9.29, 8.84, and 8.78), and four singlets attributable to the β-methyl protons (δ 3.60, 3.64, 3.68, 3.74). These results strongly suggest the presence of only one diastereomer, as a *d,l* racemate.

The formation of a particular diastereomer (either syn or anti) is determined by the orientation of the two porphyrin rings during the closure of the second amide linkage. It is therefore reasonable to assume that kinetic control in this step will lead to the less sterically hindered anti isomer. It is interesting that even with the amide synthesis employed in the coupling reaction of FTF4* (which is faster than that used for FTF4), still only one diastereomer is obtained.

Decoupling experiments allowed us to assign the doublet centered at δ 6.97 to the protons on the amide nitrogens. These studies also allowed us to assign the quadruplet centered at δ 5.8 and the doublet centered at δ 4.7 to the diastereotopic protons of the

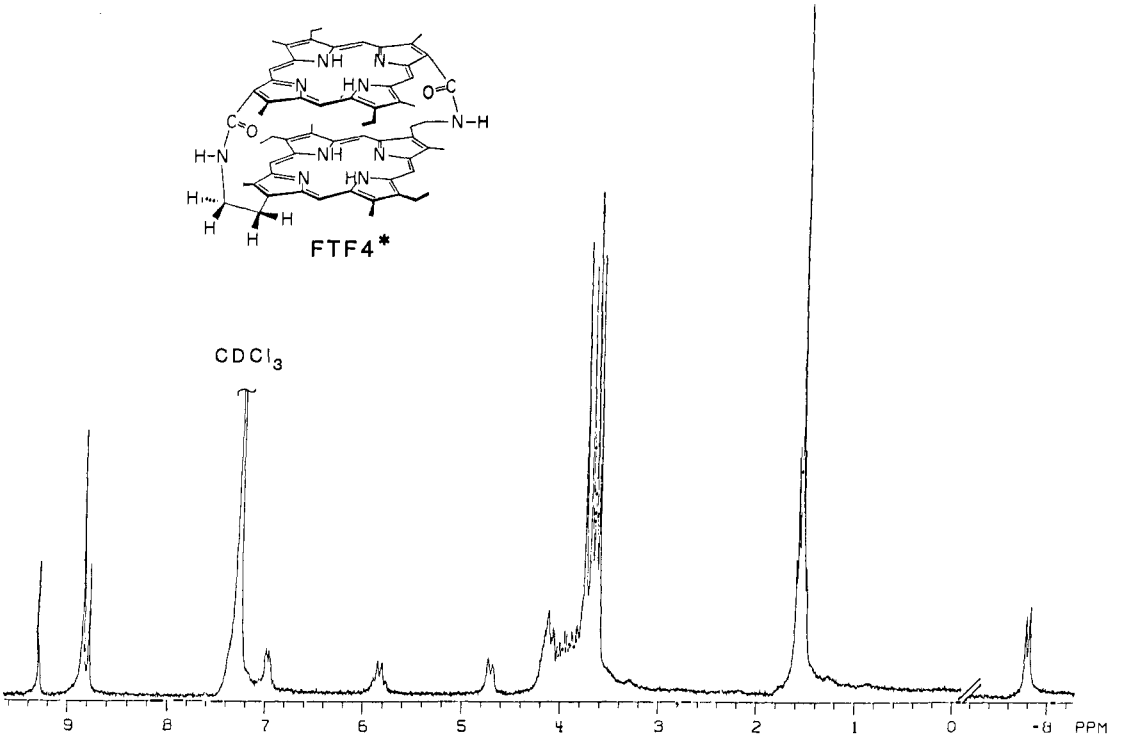

Figure 9. ^{1}H NMR spectrum of H_4(FTF4*).

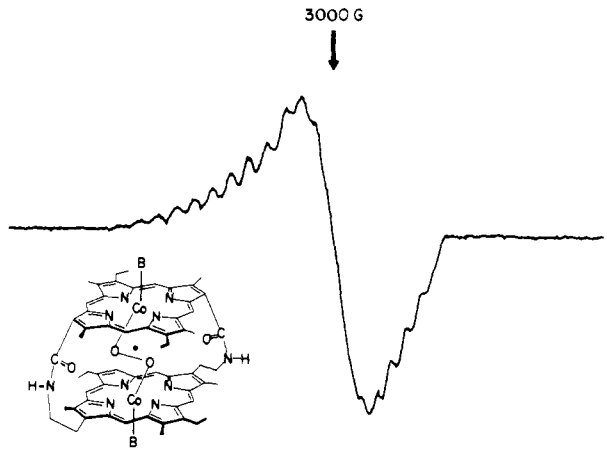

Figure 10. ESR spectrum of the superoxo derivative of Co_2(FTF4*): $g_\perp = 2.33$; $A_\perp = 16.5 \times 10^{-4}$ cm^{-1}; B = 1 MeIm.

methylene group adjacent to the NH amide groups. Irradiation at the frequency of any of these three resonances caused each of the other two multiplet peaks to collapse into singlets. The multiplet arising from the other bridging methylene adjacent to the porphyrin ring (ca. δ 4.1) overlaps with the signals corresponding to the ethyl methylene protons (δ 3.8–4.0). All the above results provide further evidence for the presence of only one diastereomer.

The resonances due to the internal pyrrolic NH protons are shifted upfield (δ −7.78, −7.81) relative to the monomeric precursors (ca. δ–4). This corroborates further the cofacial structural assignment for FTF4*.

FTF3 displays a ^{1}H NMR spectrum similar to that of FTF4*, with the exception that the resonance arising from the extra methylene groups of the FTF4* bridges (ca. δ 4.1) is missing in the FTF3 spectrum.

The internal pyrrolic NH proton signals of FTF3 are observed at higher fields than the corresponding signals for FTF4* (Table III). This shift is a result of the enhanced anisotropic shielding effect due to the smaller separation between the two macrocycles in FTF3. However, this chemical shift, which we had earlier found to be diagnostic of the relative interplanar distances,[2b] does not follow the expected systematic trend shown in Table I. It is possible that the relative orientation of the amide carbonyl groups determines whether their electronic effect will reinforce or cancel anisotropic effects of the porphyrin rings.

ESR Spectroscopy. Electron spin resonance (ESR) was used both in the characterization of the dicobalt dimers and to monitor their interaction with molecular oxygen. The ESR spectrum of Co_2(FTF4*), in a frozen glass of 1:1 toluene–CH_2Cl_2 with a 20-fold excess of 1-MeIm, exhibits a single broad transition signal, with $g_\perp = 2.33$. The parallel transition shows a poorly resolved triplet splitting due to the interaction of the nitrogeneous axial base with the cobalt centers.

Contrary to previous observations[2b] for the Co_2(FTF4) isomer, the Co_2(FTF4*) spectrum does not show a metal–metal zero-field-splitting interaction. Upon exposure to air, the above compound becomes ESR silent, probably because of formation of the diamagnetic (μ-peroxo)cobalt(III) adduct. As reported previously for Co_2(FTF4) and its analogue,[2b,17] this apparent oxygen adduct is readily oxidized by molecular iodine to give (μ-superoxo)cobalt dimer, whose ESR spectrum is displayed in Figure 10. This spectrum shows one large transition signal ($g = 2.025$) with 15 secondary absorptions, which is consistent with an unpaired electron located in the superoxobridge, interacting with the two $I = {}^7/_2$ cobalt nuclei.[18,19] It is noteworthy, however, that this spectral pattern (Figure 9) is not as isotropic as that observed for the Co_2(FTF4) μ-superoxo complex.[2b] This difference may result from overlap of the transitions for the "perpendicular" and "parallel" regions.

This small g anisotropy suggests that Co_2(FTF4*) is forming an oxygen adduct that has a different, less symmetric configuration[20] than that for Co_2(FTF4). The Co_2(FTF4*) μ-superoxo ESR spectrum is, in fact, similar to that observed for 1:1 monomeric cobalt–dioxygen, which has been attributed to a bent Co–O_2 unit (g ca. 2.08).[21] These results possibly indicate that the electron in the superoxobridge is preferentially interacting with one of the two cobalt centers.

The frozen solution in 1:1 toluene–CH_2Cl_2 of Co_2(FTF3) exhibits the same ESR spectra with and without 1-MeIm. This spectrum consists of one broad transition signal with an isotropic g factor of 2.33. It is less intense and less resolved than that for Co_2(FTF4*), but not broader. The short distance between the two porphyrin planes may allow some orbital interaction between the two cobalt centers, thus facilitating coupling between the two impaired electrons. This could give rise to singlet and triplet states, which may, in turn, explain the observed isotropic transition and the absence of M–M zero-field-splitting interaction. This interpretation is tentative. Note that the presence of axial base should ensure that O_2 coordinates to cobalt within the cavity.

When Co_2(FTF3) with a 20-fold excess of 1-MeIm was exposed to air, it became ESR silent and it remained so in this case even after I_2 addition. It seems that the two Co(II) centers were oxidized to Co(III), thus becoming diamagnetic. The lack of response upon I_2 addition suggests that a μ-superoxo Co adduct is not formed. The outer coordination sites of the cobalt centers should be blocked by the excess 1-MeIm axial ligand, and it is plausible that the interporphyrin gap is too small to allow the oxygen to enter the internal cavity.

Electrochemistry. The electrocatalytic behavior of the dicobalt derivatives of FTF3 and FTF4* in the reduction of dioxygen is described elsewhere.[8] However, for the purposes of the present discussion, it is important to note that both derivatives act to catalyze *only* the 2e reduction of O_2 to H_2O_2.

Conclusions

The difference in catalytic behavior between Co_2(FTF4) and both Co_2(FTF4*) and Co_2(FTF3) could be a result of the inability of the latter two complexes to form the Co–O_2–Co intermediate that is believed to be essential for the four-electron reduction of dioxygen.[2b] The extreme sensitivity of the catalytic activity of these porphyrin dimers to the intimate geometry of these compounds also can be understood on this basis.[4]

A CPK model of Co_2(FTF3) indicates that the interporphyrin distance is too short to allow the O_2 molecule to enter the cavity of the dimer. This seems to be corroborated by the ESR results for Co_2(FTF3), but it still remains uncertain whether O_2 can bind in the cavity. On the basis of this hypothesis, O_2 would interact only with the external coordination site on one of the two cobalt centers. In other words, dioxygen may preferentially bind on the outside of the adsorbed porphyrin dimer rather than entering the prophyrin cavity. The electroreduction of dioxygen then proceeds to hydrogen peroxide in a manner similar to that of the monomeric cobalt porphyrin catalyst.[22]

ESR studies for Co_2(FTF4*) revealed that a Co–O_2–Co adduct is formed inside the interporphyrin cavity. However, the pattern of the ESR spectrum suggests that this cobalt–oxygen complex is structurally less symmetric than that of Co_2(FTF4). In any case, Co_2(FTF4*) only catalyzes the two-electron reduction of O_2 to H_2O_2.

It is possible that the more symmetric Co–O_2–Co intermediate formed by Co_2(FTF4) adopts a specific conformation in which the dioxygen group is stabilized by the cobalt centers and one proton. Such added stability might permit the dicobalt μ-peroxo intermediate to survive long enough for its further reduction to

(17) Chang, C. K. *J. Chem. Soc., Chem. Commun.* **1977**, 800.
(18) Sykes, A. G. *Prog. Inorg. Chem.* **1970**, *13*, 1.
(19) Weil, J. A.; Kinnaird, J. L. *J. Phys. Chem.* **1967**, *71*, 3341.
(20) Pilbrow, J. R.; Lowry, M. R. *Rep. Prog. Phys.* **1980**, *43*, 433.
(21) Smith, T. D.; Pilbrow, J. R. *Coord. Chem. Rev.* **1981**, *39*, 295.
(22) Durand, R. R., Jr.; Anson, F. C. *J. Electroanal. Chem. Interfacial Electrochem.* **1982**, *134*, 273–289.

H_2O. The less symmetric dicobalt–dioxygen intermediate in FTF4* might not have the appropriate geometry to attain such stabilization so that it is hydrolyzed instead of being further reduced. This explanation must remain tentative until further studies of the coordination chemistry of the Co_2(FTF4*) are completed.

There are other structural differences between the dicobalt derivatives of FTF4 and FTF4* that could lead to a two-electron rather than a four-electron pathway. Thus, the probable tendency of the two carbonyl groups in FTF4* to be coplanar with respect to the porphyrin ring would afford a more conjugated system. This would reduce the distance between the two porphyrin rings. Such a phenomenon is suggested by examination of CPK models and is reflected in the corresponding UV–visible spectra. This structural condition could result in a Co–O_2–Co intermediate that does not meet the stringent requirements for the four-electron process.

Another consequence of this structural difference would be more rigidity in the linking bridges in FTF4*, in which the amide protons point away from the cavity. The amide protons may be playing a critical role in the stabilization of the required Co–O_2–Co intermediate for the four-electron reduction process. They would not be available in the Co_2(FTF4*) complex. Still, in the absence of detailed structural data, these suggestions are speculative.

Experimental Section

Reagents and Solvents. All reagents and solvents were of reagent-grade quality, purchased commercially, and used without further purification, except where noted below. Dry solvents were heated at reflux (over 6 h) with and distilled from CaH_2 (hexanes, methylene chloride, THF), magnesium methoxide (methanol), and P_2O_5 (toluene) under N_2. 2,6-Lutidine (Aldrich) was dried over molecular sieves and distilled under N_2 before use. Pyridine was dried over molecular sieves. Molecular sieves (Linde, $^1/_{16}$ in. pellets, size 4 Å) were activated by heating (ca. 155 °C) under vacuum overnight. Oxalyl chloride, sulfuryl chloride, and boron trifluoride etherate were distilled under nitrogen.

Physical and Spectroscopic Methods. Electronic spectra were obtained in CH_2Cl_2 solutions on a Cary 219 spectrometer. Pulsed Fourier transform ^1H NMR spectra of the free-base ligands were obtained on Varian XL-100 and 300 MHz Nicolet spectrometers using a Nicolet Technological Corp. Model 1180 FT disk data system. Mass spectral determination of FTF4*, FTF3, and their cobalt derivatives was carried out at the Middle Atlantic Mass Spectrometry Laboratory, a National Science Foundation Shared Instrumentation Facility. The MS-50 from AEI/Kratos was calibrated with 1185 triazine. High-resolution mass spectral analysis (EI) of the cobalt derivative of the C1 diethyl ester was obtained on a Finnigan MAT-311A calibrated with perfluorokerosene. X-band ESR spectra were obtained on a Varian E-12 spectrometer.

5-(*tert*-Butoxycarbonyl)-5′-(1,3-dithiolan-2-yl)-4′-(ethoxycarbonyl)-3-ethyl-4,3′-dimethyl-2,2′-dipyrromethane (16). Ethyl 2-(1,3-dithiolan-2-yl)-4-methylpyrrole-3-carboxylate (**15**) (1.0 g, 5.9 mmol)[13] and *tert*-butyl 5-(acetoxymethyl)-4-ethyl-3-methylpyrrole-2-carboxylate (**14**) (1.1 g, 3.1 mmol) were stirred together in glacial acetic acid (20 mL) containing a catalytic amount of *p*-toluenesulfonic acid at 35 °C under N_2 for 5 h.[25] Chloroform was then added (30 mL) and the mixture extracted with water (3 × 50 mL).

The organic phase was washed with aqueous sodium bicarbonate until neutral and then dried over Na_2SO_4. The dry solution was filtered through Celite, and the solvent was removed under reduced pressure to afford a yellow solid, which was recrystallized twice from aqueous ethanol to yield the product as yellow plates: mp 129–130 °C; ^1H NMR (CDCl,3) δ 1.07 (t, 3 H, methylene of β-pyrrolic ethyl), 1.38 (t, 3 H, methyl of the ethyl ester), 1.55 (s, 9 H, t-Bu), 2.21 (s, 3 H, β-pyrrolic methyl), 2.25 (s, 3 H, β′-pyrrolic methyl), 2.40 (q, 2 H, methylene of the ethyl ester), 3.14 (s, 4 H, methylenes of acetal), 3.77 (s, 2 H, methane bridge), 4.23 (q, 2 H, methylene β-pyrrole ethyl), 6.26 (s, 1 H, thioacetyl); MS, *m/e* 478 (calcd 478 for $C_{24}H_{34}C_4N_2S_2$).

5-(*tert*-Butoxycarbonyl)-5′-formyl-4′-(ethoxycarbonyl)-3-ethyl-4,3′-dimethyl-2,2′-dipyrromethane (17) (Thioacetal Deprotection). Boron trifluoride etherate (0.5 mL) was added to a stirred suspension of red mercuric oxide (65 mg) in tetrahydrofuran (10 mL) containing water (1 mL). After 10 min, thioacetal-protected dipyrromethane **16** (80 mg, 0.17 mmol) was mixed in, and the resulting deep-red solution was stirred for 15 min. After dilution with water (20 mL), aqueous sodium hydrogen sulfide (200 mg) was slowly added, and the reaction mixture was stirred until precipitation of HgS was completed.

The mixture was then filtered through Celite, and the residue was washed with THF and ether. The organic phase of the filtrates was separated, and the aqueous phase was extracted further with ether (2 × 25 mL). The organic layers were combined, washed with H_2O, and dried over $MgSO_4$. The solvent was removed by rotary evaporation, and the remaining red oil thus obtained was used directly in the subsequent porphyrin synthesis.

C1 Diethyl Ester Porphyrin 7. The dipyrromethane **17** from the above synthesis was added to stirred trifluoroacetic acid (3 mL) over 10 min. The solution was then diluted with glacial acetic acid (150 mL), and hydroiodic acid (1 mL, 56%) was added. The resulting dark solution was stirred for 1 h, followed by addition of chloroform (200 mL). The organic phase was separated, washed with aqueous sodium bicarbonate until neutral, and dried over Na_2SO_4. The solution was filtered and the filtrate stirred in an air atmosphere in the absence of light for 24 h to allow oxidation of the porphodimethane intermediate to the porphyrin product.

The chloroform was removed under reduced pressure, and the residue was dissolved in dichloromethane (50 mL) and methanol (25 mL). The solvent was slowly removed in the rotary evaporator, and the resulting crystalline porphyrin was collected.

The mother liquor was chromatographed on preparative TLC (silica), with dichloromethane as eluent. This fraction was combined with the first crop and recrystallized from CH_2Cl_2–CH_3OH. The porphyrin product **7** was obtained as purple crystals (28 mg, 24%) from the thioacetal dipyrromethane **16**: UV–vis [λ_{max} in CH_2Cl_2 (log ε)] 410 (5.38), 517 (3.83), 558 (4.27), 582 (3.99), 636 (3.39) nm; ^1H NMR ($CDCl_3$) δ −3.76 (br s, 2 H, internal pyrrole NH), 1.83 (t, 6 H, methyl of the ethyl groups), 1.88 (t, 6 H, methyl of ester), 3.70 (s, 6 H, β-pyrrole methyl), 3.94 (s, 6 H, β-pyrrole methyl), 4.89 (q, 4 H, methylene of β-pyrrole ethyl), 4.17 (q, 4 H, methylene of the ethyl ester), 10.17 (s, 2 H, meso H), 11.12 (s, 2 H, meso H); high-resolution mass spectrum of the cobalt derivative of the C1 diethyl ester porphyrin ($C_{34}H_{36}N_4O_4Co$): theoretical mass, 623.2069; measured mass, 623.2076.

C1 Diacid 8. The diester porphyrin **7** (36 mg) was added to a solution of 12 N HCl (45 mL) and CF_3COOH (15 mL). The solution was stirred at 95 °C for 24 h, under argon, with the flask covered with aluminum foil. The reaction mixture was cooled to room temperature, and solvents were removed under reduced pressure.

The solid was redissolved in CH_3OH (10 mL), and the solution was slowly neutralized with pyridine. After cooling for ca. 6 h, the crystalline product was collected by filtration, washed with CH_3OH, and dried in vacuo (24.5 mg, 78%).

C1 Bis(acid chloride) Porphyrin 9. The dicarboxylic acid porphyrin (14.20 mg, 2.78×10^{-5} mol) was stirred under argon with freshly distilled oxalyl chloride (3 mL) for 3 h. The solvent was removed under reduced pressure and the residue dried in vacuo for 1 h. Residual traces of oxalyl chloride were then removed by passing an argon flow over the solid for about 5 min. This crude bis(acid chloride) porphyrin was used immediately for the "face-to-face" coupling reaction.

Synthesis of Face-to-Face Porphyrins. General Method. One equivalent of the crude C1 bis(acid chloride) porphyrin **9** was dissolved in dry CH_2Cl_2 under argon, and the solution was loaded into a gas-tight syringe mounted on a motor-driven syringe pump (Sage Instruments Co., Model 355). A second syringe was filled with an equal volume of a solution of 1 equiv of the appropriate diaminoporphyrin in dry CH_2Cl_2 containing 0.5–1 mL of dry Et_3N.

The contents of the two syringes were then slowly pumped under argon into a three-necked, round-bottom flask containing dry dichloromethane in sufficient quantity to ensure a final concentration of porphyrin reactants of 10^{-3} M. The two reagents were simultaneously added from the syringes through Teflon tubing and rubber septa attached to the outer necks of the flask. When the addition was complete, stirring was continued until the fumes in the flask had disappeared (ca. 30 min).

The solution was filtered through Celite, and the filtrate washed with H_2O, dried over K_2SO_4, and concentrated for column chromatography on silica, with CH_2Cl_2 as eluent. The porphyrin dimer was then crystallized from CH_2Cl_2–CH_3OH.

FTF4* (5). This compound was synthesized according to the general method, using the bis(acid chloride) porphyrin **9** derived from the diacid porphyrin **8** (14.20 mg, 2.78×10^{-5} mol) and the porphyrin diamine **10** (14.15 mg, 2.78×10^{-5} mol) (synthesized as in ref 9). Addition time was 5 min. The product was chromatographically purified on a silica column (10 × 2.5 cm), with 0.5% Et_3N in CH_2Cl_2 as eluent. A narrow, faster moving band of an uncharacterized component (UV–vis suggested that it was monomeric porphyrin) was eluted first. The brownish product was isolated and crystallized from CH_2Cl–CH_3OH as purple needles (40%): ^1H NMR ($CDCl_3$) (Figure 9); UV–vis (λ_{max} in CH_2Cl_2) 372, 507, 548, 578, 640 (sh) nm; MS, *m/e* 983.5 (calcd 982.5).

FTF3 (6) was synthesized according to the general method, using the bis(acid chloride) porphyrin **9** derived from the diacid porphyrin **8** (10.35 mg, 2.03×10^{-5} mol) and the C1 porphyrin diamine **11** (9.74 mg, 2.03

× 10^{-5} mol) (synthesized as in ref 9). Isolation and purification were performed as for FTF4*; yield 30%; UV-vis (λ_{max} nm) 370, 502 (sh), 536, 566, 644; MS *m,e* 955 (calcd 954).

Cobalt insertion into FTF3 and FTF4 was performed in an inert atmosphere box, with $CoCl_2$ in 1:3 THF-toluene, as previously described in ref 9. Co_2(FTF4)*: *m/e* 1097.4 (calcd 1096.4); Co_2(FTF3): *m/e* 1069.4 (calcd 1068.3).

Acknowledgment. This work derives from a collaborative effort that also includes the groups of Professors, F. C. Anson (Caltech), M. Boudart and H. Taube (Stanford), and Dr. H. Tennet, formerly of Hercules Inc. Research Center. Mass spectral analyses were carried out at the Middle Atlantic Mass Spectrometry Laboratory, a National Science Foundation Shared Instrumentation Facility. We thank R. R. Durand, Jr., Dr. E. R. Evitt, and Dr. L. J. Wright for helpful discussions. Initial studies were carried out at Stanford by Dr. R. B. Pettman; his work is gratefully acknowledged. This project was supported by National Science Foundation Grants CHE77-22722 and CHE81-10545. Use of the Stanford Magnetic Resonance Laboratory (NSF Grant GP23633 and NIH Grant RR00711) is also acknowledged. C.S.B. thanks the Venezuelan Council for Scientific and Technological Research (CONICIT) for her doctoral fellowship. We are deeply indebted to Dr. L. Tokes (Syntex) for a high-resolution mass spectrum and to G. Venburg for technical assistance.

Registry No. 5a, 85048-67-5; **5b**, 84928-54-1; **6a**, 85048-68-6; **6b**, 84928-53-0; **7**, 85048-69-7; **8**, 85048-70-0; **9**, 85048-71-1; **10**, 85048-72-2; **11**, 85048-73-3; **14**, 82448-72-4; **15**, 51741-11-8; **16**, 85048-74-4; **17**, 85048-75-5; oxygen, 7782-44-7.

Mechanistic Aspects of the Catalytic Reduction of Dioxygen by Cofacial Metalloporphyrins

Richard R. Durand, Jr.,[†] C. Susana Bencosme,[‡] James P. Collman,*[‡] and Fred C. Anson*[†]

Contribution from the Arthur Amos Noyes Laboratory, Division of Chemistry and Chemical Engineering,[§] California Institute of Technology, Pasadena, California 91125, and Department of Chemistry, Stanford University, Stanford, California 94305. *Received August 2, 1982*

Abstract: The mechanisms by which the reduction of dioxygen at graphite electrodes is catalyzed by cofacial dicobalt and related porphyrins adsorbed on the electrode surface have been scrutinized. The products of the reduction, the electrode potential where the reduction proceeds, and the mechanistic role of protons were among the topics examined. For the best catalyst it was possible to relate the electrochemical response of the adsorbed porphyrin to the potential where the catalyzed reduction of dioxygen proceeds. The electrocatalytic behavior of several new heterobinuclear cofacial porphyrins is reported as well as that of a new cofacial dicobalt porphyrin in which the bridge connecting the two porphyrin rings consists of only three atoms. A comparison of the behavior of the various catalysts has led to a more detailed proposal for the mechanisms by which they operate in catalyzing the electroreduction of dioxygen.

In previous accounts of the unusual catalytic potency of several dicobalt cofacial porphyrin molecules for the electroreduction of dioxygen to water,[1-3] the catalytic mechanism was surmised on the basis of limited experimental data. In particular, the reduction and oxidation of the catalysts themselves in the absence of O_2 were difficult to observe above the background response from the surface of the pyrolytic graphite electrode on which they were adsorbed. The effects of changes in the proton concentration on the catalysis were also examined only cursorily although it was shown that the course of the reduction was substantially different at electrodes deprived of protons.[1-3]

We have now found conditions that permit the electrochemical responses of the adsorbed catalysts to be observed clearly and reproducibly both in the absence and in the presence of O_2 and over a wide pH range. The rate constant for the first step in the catalytic reaction has been measured, and the effect of pH on the distribution of reduction products between H_2O_2 and H_2O has been determined. The catalytic activities of dicobalt cofacial porphyrins with six, five, four, and three atoms in the amide bridges have been compared, and the behavior of several new heterobinuclear cofacial porphyrins (Figure 1) has been examined. The results obtained have provided new insight into the mechanisms employed by these catalysts in reducing dioxygen.

Experimental Section

Materials. The detailed synthetic procedures employed to obtain the metalloporphyrin molecules utilized in this study are presented elsewhere.[4] Figure 1 lists the porphyrins employed and the abbreviations used to identify them. Pyrolytic graphite electrodes were obtained and mounted as previously described.[5] Reagent-grade chemicals and solvents were used as received. The electrodes were mounted to expose the edges rather than the basal planes of the pyrolytic graphite. Such edge-plane electrodes cannot be cleaved to renew the electrode surface so their surfaces were prepared by polishing with 600-grade SiC paper (3M Co.).

Procedures. Pyrolytic graphite electrodes were coated with porphyrin catalysts by syringing small volumes of stock solutions in dichloroethane onto the electrode surface and allowing the solvent to evaporate. Coulometric assays of the resulting coatings performed by measuring the areas under cyclic voltammograms recorded in the absence of dioxygen showed that they typically contained 2-4 × 10^{-10} mol cm^{-2}, which corresponds to a few close-packed monolayers on a smooth surface or to a single monolayer on a graphite surface with a roughness factor of 2-3. This quantity of adsorbed electroactive catalyst was reproducibly ob-

[†] California Institute of Technology.
[‡] Stanford University.
[§] Contribution No. 6683.

(1) Collman, J. P.; Marrocco, M.; Denisevich, P.; Koval, C.; Anson, F. C. *J. Electroanal. Chem. Interfacial Electrochem.* **1979**, *101*, 117-122.
(2) Collman, J. P.; Denisevich, P.; Konai, Y.; Marrocco, M.; Koval, C.; Anson, F. C. *J. Am. Chem. Soc.* **1980**, *102*, 6027-6036.
(3) Collman, J. P.; Anson, F. C.; Bencosme, S.; Chong, A.; Collins, T.; Denisevich, P.; Evitt, E.; Geiger, T.; Ibers, J.; Jameson, G.; Konai, Y.; Koval, C.; Meier, K.; Oakley, R.; Pettman, R.; Schmittou, E.; Sessler, J. In "Organic Synthesis, Today and Tomorrow", Trost, B. M., Hutchinson, C. R., Eds.; Pergamon Press: New York, 1981; pp 29-45.
(4) (a) Collman, J. P.; Anson, F. C.; Barnes, C. E.; Bencosme, C. S.; Geiger, T.; Evitt, E. R.; Kreh, R. P.; Meier, K.; Pettman, R. B. *J. Am. Chem. Soc.*, first of four papers in this issue. (b) Collman, J. P.; Bencosme, C. S.; Durand, R. R., Jr.; Kreh, R. P.; Anson, F. C. *Ibid.*, second of four papers in this issue. (c) Collman, J. P.; Bencosme, C. S.; Barnes, C. E.; Miller, B. D.; *Ibid.*, third of four papers in this issue.
(5) Durand, R. R., Jr.; Anson, F. C. *J. Electroanal. Chem. Interfacial Electrochem.* **1982**, *134*, 273-289.

0002-7863/83/1505-2710$01.50/0